APPENDIX A

Rock Scour

George W. Annandale and Erik F. R. Bollaert

INTRODUCTION

Rock scour can occur when the erosive capacity of water exceeds the ability of rock to resist it. Typical environments where rock scour is a concern are downstream of overtopping dams, downstream of spillways, in plunge pools, around bridge piers, in unlined rock tunnels, and in channels and at other structures constructed in rivers and marine environments. Development of technology to predict scour of rock commenced in 1991 and has seen significant growth since then.

This appendix provides a summary of technology that can be used to determine the potential for and the extent and rate of rock scour. The latest technology in this field is explained in more detail in Schleiss & Bollaert (2002) and in Annandale (2006). Both works provide a detailed exposition of rock scour technology, explains methods for applying it, and provides a number of case studies validating the technology and demonstrating its application.

Two quantitative approaches, known as the Erodibility Index Method (EIM; Annandale 1995, 2006) and the Comprehensive Scour Model (Bollaert 2002, 2004; Bollaert & Schleiss 2005), can be used to predict the potential for and the extent of scour. While both approaches allow estimating the ultimate possible scour depth, only the latter model is capable of predicting scour evolution as a function of time. By following these approaches, the practitioner can cross-check results and identify failure modes leading to scour of rock.

The EIM is basically a semi-empirical model that is based on a scour threshold relating the relative magnitude of the erosive capacity of water to the relative ability of rock to resist it (Annandale 1995). When using this method, the relative ability of rock to resist erosion is quantified by a geomechanical index known as the erodibility index. The erosive capacity of water is determined by quantifying the stream power of the flowing water. The universality of the scour threshold relationship offered by the EIM and the use of stream power to quantify the relative magnitude of the erosive capacity of water provide practitioners with the ability to solve almost any scour problem in a global manner (Annandale 2006) for its ultimate depth. No rate of scour is available, however.

The Comprehensive Scour Model (CSM) developed by Bollaert (2002, 2004) is a completely physically based model that consists of two principal components: the comprehensive fracture mechanics (CFM) method and the dynamic impulsion (DI) method. Application of the CFM is focused mainly on fissured rock where brittle fracture or failure by fatigue dominates. Brittle fracture occurs instantaneously, while failure by fatigue is time dependent and thus allows estimating the time evolution of scour formation. The DI method is used principally to assess scour of intact blocks of rock formed by joints and fractures, but can also be used to predict sudden failure of concrete slab linings of stilling basins (Bollaert, 2004b). In some cases, large blocks of rock delineated by joints and fractures may also contain fissures within the principal mass of the rock and all three failure mechanisms; that is, brittle fracture, failure by fatigue, and removal by dynamic impulsion may be relevant. Application of both the CFM and the DI method requires quantification of the mean and fluctuating dynamic pressures acting within fissures, joints, and fractures. These pressures are caused by turbulence in flowing water. The method can in principle be applied to any type of turbulent flow situation and any type of fractured media, provided that turbulent pressure fluctuations and the strength of the fractured media can be reasonably estimated. The model not only provides the ultimate scour depth but also an estimate of the rate of scour during the lifetime of the structure in question.

OVERVIEW OF ROCK SCOUR

Rock scour occurs when the erosive capacity of water flowing over the rock exceeds its ability to resist scour. It is therefore

necessary to not only understand the characteristics of flowing water leading to scour of rock but also devise practical methods to quantify its erosive capacity. Similarly, it is necessary to investigate and understand the failure mechanisms in rock leading to scour and devise practical approaches for quantifying its ability to resist the erosive capacity of water. A relationship between the erosive capacity of water and the ability of rock to resist it at the threshold of motion is known as a scour or erosion threshold.

Erosive Capacity of Water

Most engineers interested in the interaction between flowing water and earth materials opine that the shear stress exerted by the flowing water on the material results in erosive action. Bollaert (2002) proves that the erosive capacity of turbulent flow on fractured rock is the result of fluctuating pressures and not shear stress, while Annandale (2006) demonstrates that use of shear stress is correct for laminar flow only. These are important observations, as application of a shear stress concept cannot explain how large blocks of rock can be removed from a rock formation or how turbulent flow can break rock blocks into smaller pieces.

To state this, Bollaert (2002) and Bollaert and Schleiss (2003; 2005) conducted detailed research into pressure fluctuations of turbulent plunging jets and determined how these pressure fluctuations interact with rock joints and fissures. They developed methods that can be used to quantify the relative magnitude of fluctuating pressures due to turbulent jet flows, which are very useful when investigating scour of rock in plunge pools or stilling basins downstream of hydraulic structures. They also showed that free air in the water can play a significant role in causing resonance of fluctuating pressures in close-ended rock fissures, increasing pressure magnitudes by up to 20 times. Such amplification plays an important role when rock scour occurs because of brittle fracture or fatigue failure. Bollaert (2002) also showed that block removal by dynamic impulsion occurs because of the transient effect of pressure waves introduced into rock joints and depends on the time persistency of the net uplift forces.

Pragmatic methods to quantify the relative magnitude of fluctuating pressures due to turbulent flow (Fig. A-1) are available for turbulent jets, hydraulic jumps and horizontal and vertical river constrictions, such as for example bridge abutments or bed sills (Hoffmans & Verheij, 1997). Other flow situations such as bridge piers are currently under investigation. For flow scenarios where the turbulence intensity of the flow cannot be readily estimated, indirect techniques can be used to quantify the relative magnitude of pressure fluctuations. Annandale (1995) used a direct relationship between stream power and the relative magnitude of turbulent pressure fluctuations. The other approach relies on findings by Hinze (1975), that is, that the magnitude of fluctuating pressures can be correlated to boundary shear stress caused by flowing water.

Stream power is equivalent to the rate of energy dissipation in flowing water, which is high when flow is very turbulent and decreases when flow is less turbulent. Turbulence in flowing water is the principal reason for energy dissipation.

A general expression for stream power is

$$SP = \int_{x2}^{x1} \rho\, g \cdot Q \cdot \Delta E(x) \cdot dx \tag{A-1}$$

where
SP = total stream power between locations x_1 and x_2;
t = time;
$\Delta E(x)$ = energy head loss of flow at location x;
Q = discharge;
ρ = mass density of water;
g = acceleration due to gravity.

Equation (A-1) is often of little use to most practitioners, who wish to have simple techniques to quantify the magnitude of stream power. Annandale (2006) has developed a suite of equations allowing practitioners to quantify stream power for varying flow conditions, including plunging jets, hydraulic jumps, flow around bends, flow around bridge piers, flow in tunnels and over knickpoints, as well as flow in channels.

Alternatively, should a practitioner be interested in estimating the relative magnitude of pressure fluctuations, and the shear stress exerted by the flowing water is already known, the following equations can be used. Hinze (1975) found that the root mean square of fluctuating pressures in turbulent flowing water can be correlated to the shear stress as

$$p' = 3 \cdot \tau \tag{A-2}$$

where p' = root mean square of the turbulent fluctuating pressures; τ = boundary shear stress.

In addition to this one also wishes to know the magnitude of the maximum pressure peaks that can result due to turbulence. Emmerling (1973) found that the maximum pressure peaks can be as high as $6 \cdot p'$; that is,

$$p_{\max} = 18 \cdot \tau \tag{A-3}$$

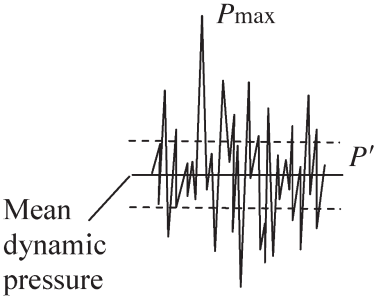

Fig. A-1. Mean dynamic pressure, root mean square of the fluctuating dynamic pressure, and maximum fluctuating dynamic pressure in turbulent flow.

An important observation when applying either of Equations (A-2) or (A-3) is that these are merely simple correlations relating pressure fluctuations to shear stress. It does not mean that scour is caused by shear but merely is a procedure to estimate the relative magnitude of pressure fluctuations if shear stress is known.

Rock Scour Mechanisms

Rock can scour by means of four mechanisms: block removal, brittle fracture, subcritical failure, and abrasion.

- Block Removal

Fluctuating pressure magnitudes resulting from turbulent flow vary as a function of space and time. The pressures introduced into rock joints due to turbulent flow can result in increased pressure directly underneath the rock. When upward pressure underneath the rock exceeds the weight of the rock block and the friction forces along its sides, the rock will start being removed from the rock formation (Fig. A-2). Depending on the time persistency of the uplift forces, this phenomenon can lead to imminent failure and occurs as soon as the upward forces exceed the downward forces for a minimum time duration (Bollaert 2002, 2004b). An example of uplift failure of concrete slabs has been observed at Gebidem Dam (Switzerland).

- Brittle Fracture

Brittle fracture of rock occurs when the stress intensity at the edges of close-ended fissures, resulting from the introduction of fluctuating pressures into the fissures, is greater than the fracture toughness of the rock (Bollaert, 2002, 2004a). When this occurs the rock fails in an explosive manner (Fig. A-3). Such failure typically results in the rock breaking up into smaller pieces. An example of rock scour by brittle fracture has been found at Santa Luzia Dam, Portugal (Annandale 2006). This failure type occurs instantaneously.

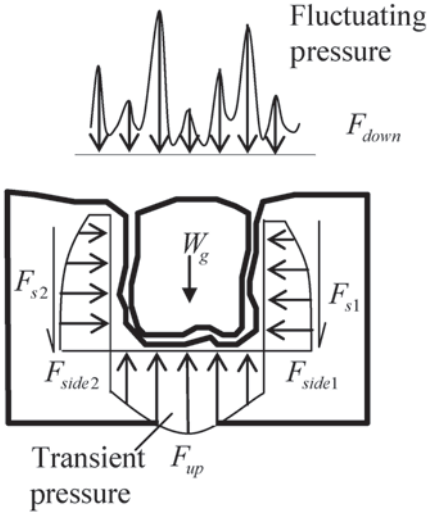

Fig. A-2. Rock scour by block removal (also known as dynamic impulsion) (based on Bollaert 2002).

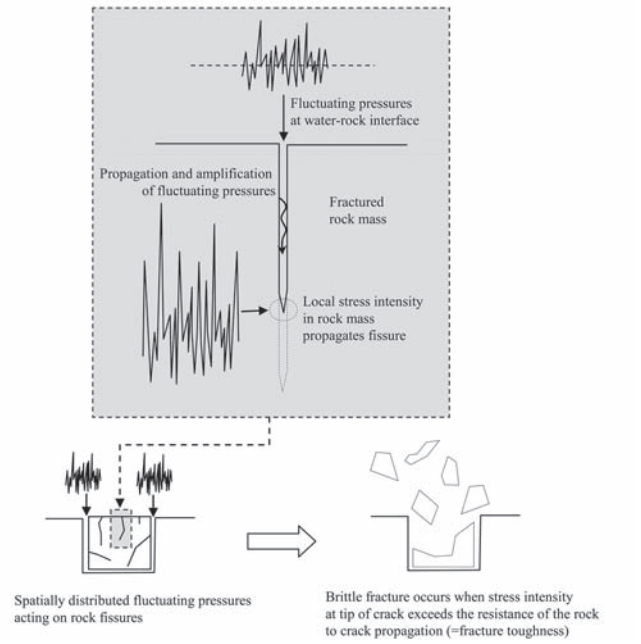

Fig. A-3. Scour of rock by brittle fracture (based on Bollaert 2002, 2004a).

- Subcritical Failure

Scour of rock by subcritical failure occurs when the stress intensities at the edges of close-ended fissures do not exceed the fracture toughness of the rock. Continued application of the fluctuating pressures in the close-ended rock fissures eventually results in breakup of the rock due to fatigue (Fig. A-4). This failure type is time dependent and both theory and practical implementations have been extensively described by Bollaert (2002, 2004a) and Bollaert and Schleiss (2005). An example of subcritical failure is the well-known scour at Kariba Dam in Zambia-Zimbabwe (Bollaert 2005).

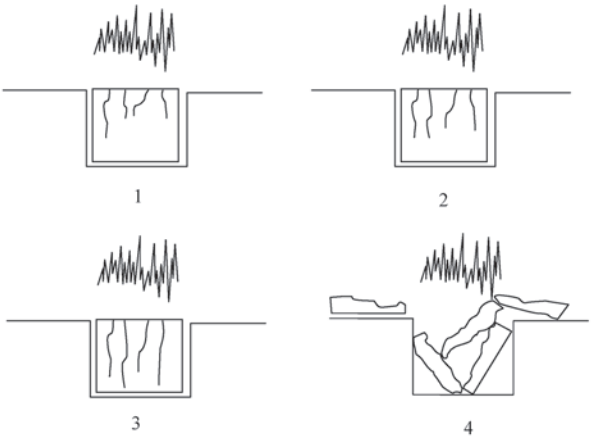

Fig. A-4. Rock scour by subcritical failure, also known as fatigue failure (based on Bollaert 2002, 2004a; Bollaert & Schleiss 2005).

- Abrasion

Scour by abrasion can occur if the fluid interacting with the rock is abrasive enough relative to the resistance offered by the rock to cause it to scour in a layer-by-layer fashion. An example of abrasion damage on concrete slabs has been observed at Gebidem Dam (Switzerland).

COMBINED APPLICATION OF METHODS

Rock scour by abrasion can currently only be analyzed by making use of laboratory testing. This type of scour is currently believed to be less prevalent than scour by sudden block removal (dynamic impulsion), brittle fracture, and fatigue failure (subcritical failure). The latter three scour mechanisms can be separately analyzed by making use of the CSM developed by Bollaert (2002, 2004), while the EIM only provides a global assessment of rock scour.

It has been found that scour analyses using the EIM and the CSM respectively provide comparable global results (Bollaert 2002; Bollaert and Annandale, 2004; George and Annandale, 2006). Comparison leads to the conclusion that the EIM predicts scour in a global manner, inherently accounting for all possible mechanisms of break-up but without any noticeable insight into which mechanism is most feasible. On the other hand, the CSM allows a much more detailed description of the type of scour as well as the scour rate.

Knowledge of how scour will occur is important for development of economical design solutions. For example, if a rock scour analysis concludes that scour will occur by brittle fracture and dynamic impulsion only, it is necessary to develop mitigation measures to protect against scour. If, in another case, an analysis indicates that scour will occur by subcritical failure (fatigue) only, it might not be necessary to design mitigation measures. This might be the case if it is found that the rock will only scour after, say, 30 days of continuous submission to fluctuating pressures. If the design flood would only submit the rock to, say, 10 hours of fluctuating pressures, the rock is unlikely to experience damage during such a flood, and protection against scour may not be warranted.

THE EIM

Hydraulic erodibility of natural and engineered earth materials can be evaluated in terms of a rational correlation between the stream power of flowing water and a geomechanical index. The relative ability of earth materials to resist scour can be characterized in terms of an erodibility index, *K*. The parameters of the index represent key material properties including mass strength, block/particle size, discontinuity/interparticle bond shear strength, and shape and orientation relative to flow. The relative magnitude of erosive power of flowing water as used in this method is represented by the stream power of flowing water.

Annandale (1995) developed a scour threshold relationship based on this approach by analyzing 137 field observations of spillway performance collected by the U.S. Department of Agriculture; observations at Bartlett Dam, Salt River Project, Arizona; and at four South African dams and published data related to initiation of sediment motion. This threshold relationship was established for a wide range of earth materials, ranging from noncohesive granular soils, cohesive soils, vegetated soils, and rock. The information presented in this appendix focuses on the erodibility of rock only. Application of this method to solve scour of other earth materials is discussed in Annandale (2006).

The observation that turbulence in flowing water is related to both energy loss and pressure fluctuations provides a convenient way to quantify the relative magnitude of the erosive capacity of water. This can be done by calculating the rate of energy dissipation (also referred to as stream power in this appendix), which has been shown to correlate to the relative magnitude of pressure fluctuations (Annandale 1995, 2006).

The correlation between rate of energy dissipation (P) and a material's resistance to erosion ($f(K)$) can be expressed by the function

$$P = f(K) \tag{A-4}$$

at the scour threshold. If $P > f(K)$, the scour threshold is exceeded, and the material is expected to erode. Conversely, if $P < f(K)$, the erodibility threshold is not exceeded, and erosion is not expected. The relationship between stream power and the Erodibility Index K is presented in Figure A-5. The data shown on the figure represent events that experience scour when subjected to flowing water and events that did not experience scour. The relationship between these values indicates a region that separates events that experienced scour from those that did not experience scour. The dashed line in this region indicates the possible location of the erosion threshold. When assessing rock scour potential, this graph is used to relate stream power to the relative ability of the rock to resist scour. If the relationship between stream power and the erodibility index for a case under consideration is located above the erosion threshold line, it is concluded that scour could occur. Alternatively, if it is located below the threshold line, it is concluded that scour is unlikely. Methods to quantify the relative magnitude of the erosive capacity of water and the relative ability of rock to resist scour are presented in the following sections.

Stream Power

A primary objective in the development of a method to calculate the relative magnitude of the erosive power of water associated with the EIM is to select parameters that reasonably represent the relative magnitude of the fluctuating pressures causing scour that can concurrently be calculated with ease. Rate of energy dissipation (or stream power) is such a parameter, and its selection can be justified per the following

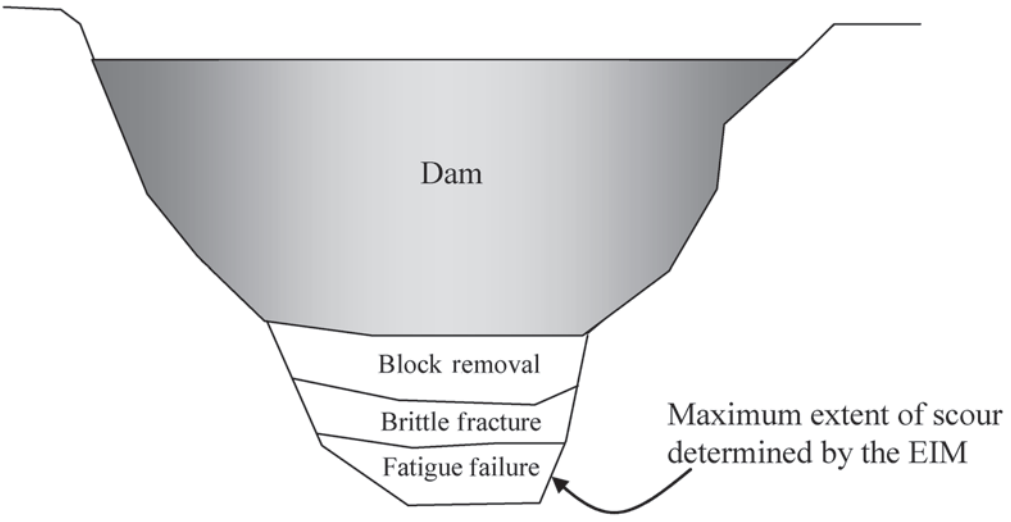

Fig. A-5. Example of scour estimation at a dam foundation resulting from overtopping by combined use of the EIM and CSM methods. Both methods are used to calculate the total scour extent. The CSM method moreover identifies the scour type (i.e., whether scour occurs by block removal, brittle fracture or fatigue failure) as well as the rate of scour.

reasoning. Turbulence causes both pressure fluctuations and energy loss, and increases in turbulence intensity concurrently result in increased rates of energy dissipation and increases in the magnitude of peak fluctuating pressures. Estimates of the rate of energy dissipation could therefore be expected to represent the relative magnitude of fluctuating pressure and thus the erosive power of the water.

Annandale (2006) presents a suite of equations to calculate the rate of energy dissipation for various flow conditions encountered in practice, including headcut formation, hydraulic jumps, channel grade change, and open channel flow. All these equations are based on a general equation that represents the rate of energy dissipation per unit area. If the energy loss is ΔE per unit length of flow (L), the unit discharge is q, average flow velocity is v, and flow depth is D, the rate of energy dissipation per unit area of the channel bed can be expressed as

$$P = \gamma \cdot q \cdot \Delta E / L = \gamma \cdot v \cdot D \cdot S_f = \tau \cdot v \tag{A-5}$$

where τ = shear stress, S_f = energy slope.

The equations for particular flow conditions are not repeated in this appendix but can be found in the cited reference.

Erodibility Index

The erodibility index K (Eq. [A-6]) represents a measure of an earth material's resistance to erosion. The index is based on Kirsten's ripability index, for which a rational relationship was established between flywheel power of excavation equipment and the ripability of earth materials (Kirsten 1982, 1988). The primary geological parameters that are used to calculate the erodibility index are mass strength, rock block size, discontinuity/interparticle bond shear strength, and shape and orientation of rock blocks relative to the direction of flow. The index is calculated as

$$K = M_s \cdot K_b \cdot K_d \cdot J_s \tag{A-6}$$

where M_s = mass strength number, K_b = block size number, K_d = discontinuity shear strength number, and J_s = relative ground structure number. All parameters can be assessed rapidly in the field by using simple identification tests and measurements. The paper by Kirsten (1982) provides standard tables quantifying these geological parameters that are also presented in Tables A-1 through A-5.

The value of M_s for rock can be determined by equating it to the unconfined compressive strength (UCS) in megapascal (MPa) if the strength is greater than 10 MPa and equal to $0.78 \times UCS^{1.05}$ when the strength is less than 10 MPa and then multiplying it with the coefficient of relative density. The latter is the ratio of a material's unit weight over 27.0 kN/m^3. Alternatively, if the unconfined compressive strength is unknown, field descriptions of the rock can be used to select values of M_s from Table A-1.

The block size number, K_b, is calculated as follows:

$$K_b = \frac{RQD}{J_n} \tag{A-4}$$

where RQD = rock quality designation, a standard parameter in drill core logging (Deere and Deere 1988), and J_n = the joint set number, which is a function of the number of joint sets in a rock mass (Table A-2). K_b ranges between 1 and 100 for rock.

Table A-1 Mass Strength Number for Rock (M_s)

Hardness	Identification in profile	Unconfined compressive strength (MPa)	Mass strength number (M_s)
Very soft rock	Material crumbles under firm (moderate) blows with sharp end of geological pick and can be peeled off with a knife; is too hard to cut tri-axial sample by hand.	Less than 1.7 1.7–3.3	0.87 1.86
Soft rock	Can just be scraped and peeled with a knife; indentations 1 mm to 3 mm show in the specimen with firm (moderate) blows of the pick point.	3.3–6.6 6.6–13.2	3.95 8.39
Hard rock	Cannot be scraped or peeled with a knife; handheld specimen can be broken with hammer end of geological pick with a single firm (moderate) blow.	13.2–26.4	17.70
Very hard rock	Handheld specimen breaks with hammer end of pick under more than one blow.	26.4–53.0 53.0–106.0	35.0 70.0
Extremely hard rock	Specimen requires many blows with geological pick to break through intact material.	Larger than 212.0	280.0

Table A-2 Joint Set Number J_n

Number of joint sets	Joint set number (J_n)
Intact, no or few joints/fissures	1.00
One joint/fissure set	1.22
One joint/fissure set plus random	1.50
Two joint/fissure sets	1.83
Two joint/fissure sets plus random	2.24
Three joint/fissure sets	2.73
Three joint/fissure sets plus random	3.34
Four joint/fissure sets	4.09
Multiple joint/fissure sets	5.00

The discontinuity or interparticle shear strength number, K_d, is determined by the ratio J_r/J_a, where J_r = joint roughness number and J_a = joint alteration number. Joint roughness refers to the roughness condition of the facing walls of a discontinuity. The joint alteration number reflects the weathering condition of the joint face material. Shear strength of a discontinuity is directly proportional to the shear strength of the gouge and inversely proportional to the degree of alteration of the joint wall material. Values for the joint roughness and joint alteration numbers are found in Tables A-3 and A-4.

In addition to representing the effective dip of the least favorable discontinuity with respect to the flow, the relative ground structure number, J_s, accounts for the shape of the material units that affects the ease with which the stream can penetrate the ground and dislodge individual units. The effective dip is the apparent dip of a discontinuity adjusted for the slope of the stream channel relative to the direction of flow. Table A-5 contains values of the relative ground structure number for various ratios of joint spacing.

Scour Assessment

The extent (depth) of scour is determined by comparing the stream power that is *available* to cause scour with the stream power that is *required* to scour the earth material under consideration. The available stream power represents the erosive power of the water discharging over the earth material, whereas the required stream power is the stream power that is required by the earth material for scour to commence. If the available stream power is exactly equal to the required stream power, the material is at the threshold of erosion. In cases where the available stream power exceeds the required stream power, the material will scour. It the available stream power is less than the required stream power, the rock will remain intact.

Figure A-7 shows how the available and required stream power, both plotted as a function of elevation beneath the original ground surface, are compared to determine the extent of scour. Scour will occur when the available stream power exceeds the required stream power. Once the maximum scour elevation is reached the available stream power is less than the required stream power, and scour ceases.

The required stream power is determined by first indexing geologic core or borehole data. The values of the erodibility index thus determined will vary as a function of elevation, dependent on the variation in material properties. Once the index values at various elevations are known, the required stream power is determined from Figure A-6. The available stream power is calculated as a function of elevation by making use of methods presented in Annandale (2006).

THE CSM

Bollaert (2002, 2004) developed a physically based engineering model for prediction of the ultimate scour depth of fissured

Table A-3 Joint Roughness Number J_r

Joint separation	Condition of joint	Joint roughness number
	Discontinuous joints/fissures	4.0
	Rough or irregular, undulating	3.0
Joints/fissures tight or closing during excavation	Smooth undulating	2.0
	Slickensided undulating	1.5
	Rough or irregular, planar	1.5
	Smooth planar	1.0
	Slickensided planar	0.5
Joints/fissures open and remain open during excavation	Joints/fissures either open or containing relatively soft gouge of sufficient thickness to prevent joint/fissure wall contact on excavation	1.0
	Shattered or microshattered clays	1.0

Table A-4 Joint Alteration Number J_a

Description of gouge	Joint alteration number (J.) for joint separation (mm)		
	1.0[1]	1.0–5.0[2]	5.0[3]
Tightly healed, hard, nonsoftening impermeable filling	0.75	—	—
Unaltered joint walls, surface staining only	1.0	—	—
Slightly altered, nonsoftening, noncohesive rock mineral or crushed rock filling	2.0	2.0	4.0
Nonsoftening, slightly clayey noncohesive filling	3.0	6.0	10.0
Nonsoftening, strongly overconsolidated clay mineral filling, with or without crushed rock	3.0*	6.0**	10.0
Softening or low friction clay mineral coatings and small quantities of swelling clays	4.0	8.0	13.0
Softening moderately overconsolidated clay mineral filling, with or without crushed rock	4.0*	8.0**	13.0
Shattered or microshattered (swelling) clay gouge, with or without crushed rock	5.0*	10.0**	18.0

Notes:

[1] Joint walls effectively in contact.

[2] Joint walls come into contact after approximately 100-mm shear.

[3] Joint walls do not come into contact at all on shear.

[4] ** Also applies when crushed rock occurs in clay gouge without rock wall contact.

Table A-5 Relative Ground Structure Number J_s

Dip direction of closer spaced joint set (degrees)	Dip angle of closer spaced joint set (degrees)	Ratio of joint spacing, r			
		1:1	1:2	1:4	1:8
180/0	90	1.14	1.20	1.24	1.26
	89	0.78	0.71	0.65	0.61
	85	0.73	0.66	0.61	0.57
	80	0.67	0.60	0.55	0.52
	70	0.56	0.50	0.46	0.43
	60	0.50	0.46	0.42	0.40
In direction of stream flow	50	0.49	0.46	0.43	0.41
	40	0.53	0.49	0.46	0.45
	30	0.63	0.59	0.55	0.53
	20	0.84	0.77	0.71	0.67
	10	1.25	1.10	0.98	0.90
	5	1.39	1.23	1.09	1.01
	1	1.50	1.33	1.19	1.10
0/180	0	1.14	1.09	1.05	1.02
	-1	0.78	0.85	0.90	0.94
	-5	0.73	0.79	0.84	0.88
	-10	0.67	0.72	0.78	0.81
	-20	0.56	0.62	0.66	0.69
	-30	0.50	0.55	0.58	0.60
Against direction of stream flow	-40	0.49	0.52	0.55	0.57
	-50	0.53	0.56	0.59	0.61
	-60	0.63	0.68	0.71	0.73
	-70	0.84	0.91	0.97	1.01
	-80	1.26	1.41	1.53	1.61
	-85	1.39	1.55	1.69	1.77
	-89	1.50	1.68	1.82	1.91
180/0	-90	1.14	1.20	1.24	1.26

Notes:
[1] For intact material, take $J_s = 1.0$
[2] For values of r greater than 8, take J_s as for $r = 8$.

and jointed rock. The CSM incorporates two major failure modes of fissured and jointed rock. The first mode, described by the comprehensive fracture mechanics (CFM) method, determines the ultimate scour depth by expressing instantaneous or time-dependent crack propagation. The second mode, described by the dynamic impulsion (DI) method, determines ultimate scour depth by calculation of the ejection of rock blocks due to sudden net uplift impulsions. The CFM method is applied principally to fissured rock and the DI method to jointed rock. However, individual rock blocks in a jointed rock mass can contain fissures that can fail in brittle fracture or by fatigue, which can lead to formation of smaller rock blocks that can be removed by dynamic impulsion with less effort. Hence, both methods are strongly related to each other.

The structure of the CSM, specifically developed for predicting scour by plunging or submerged jets, distinguishes between three modules: the falling jet, the plunge pool, and the rock mass. The latter module allows simulation of the previously mentioned failure mechanisms, that is, brittle fracture, failure by fatigue, and dynamic impulsion. Emphasis is placed on the description of physical parameters that are necessary to accurately describe the different processes. This is presented in a way that allows practicing engineers to implement the concepts while still honoring the basic principles of physics.

The Module of the Falling Jet

This module describes how the hydraulic and geometric characteristics of the jet are transformed from its point of issuance from the dam down to the plunge pool (Figure A-8). Three main parameters characterize the jet at issuance: the velocity V_i, the diameter (or thickness) D_i, and the initial jet turbulence intensity Tu (Bollaert, 2004a).

The trajectory calculation for the jet through the atmosphere is based on ballistics and drag forces encountered by the jet as it plunges through the air and will not be further outlined herein. The basic output is the impingement

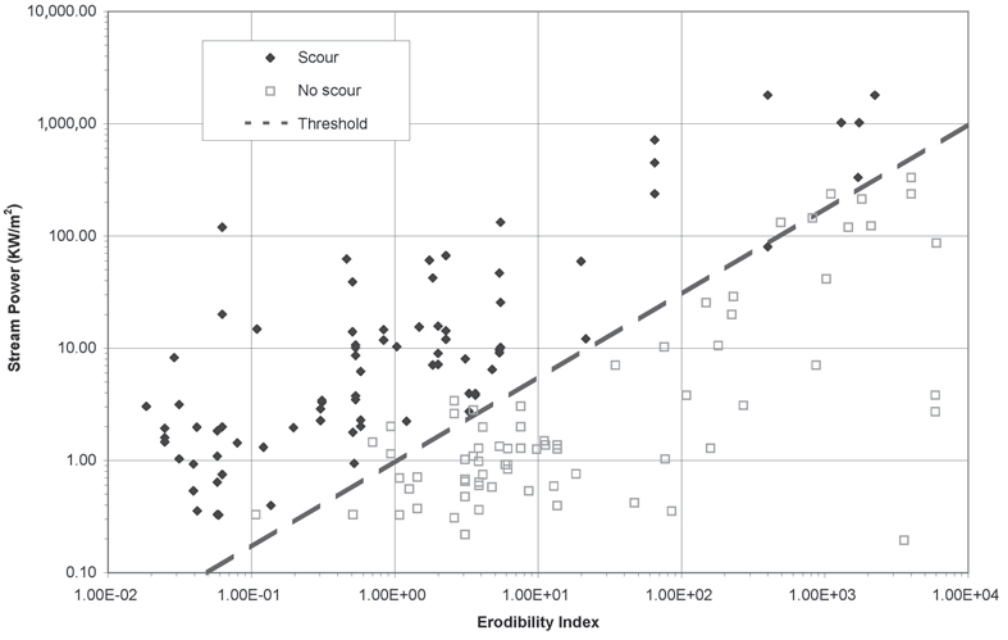

Fig. A-6. Scour threshold relating stream power and the Erodibility Index (Annandale 1995).

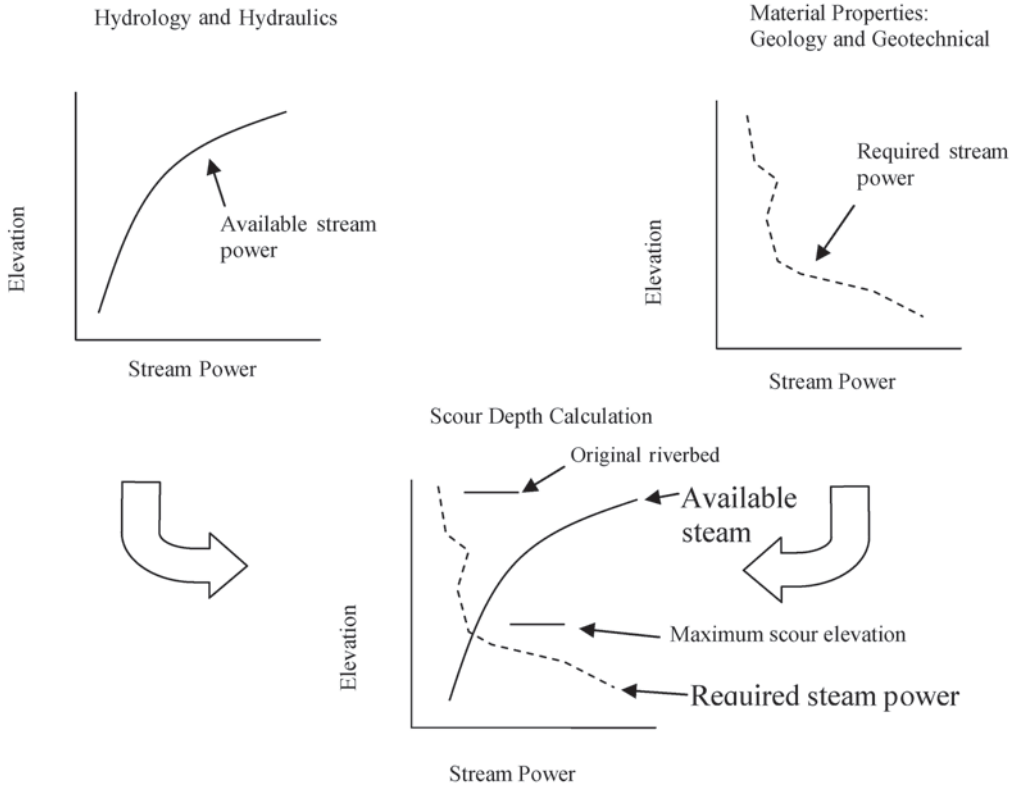

Fig. A-7. Determination of the extent of scour by comparing available and required stream power.

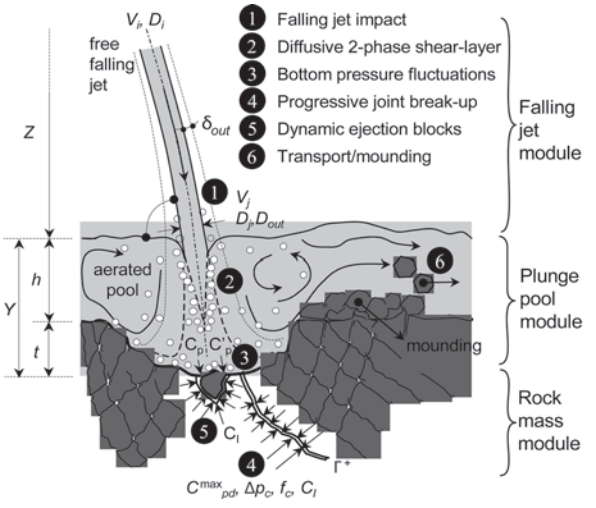

Fig. A-8. Definition sketch of the main parameters of a free overfall jet plunging into a pool and breaking up the rock mass (Bollaert 2004a).

location of the jet at impact, the jet trajectory length *L,* and the jet velocity at impact V_j. Knowledge of the jet trajectory length *L* is used to determine the contraction of the jet due to gravitational acceleration. This allows calculation of the jet diameter or thickness at impact D_j. This diameter is essential to determine the Y/D_j ratio in the plunge pool.

Second, the turbulence intensity Tu defines the lateral spread of the jet δ_{out} (Eq. [7]; Ervine et al. 1997). Superposition of the outer spread to the initial jet diameter D_i results in the outer jet diameter D_{out}, which is used to determine the extent of the zone at the water–rock interface where severe pressure damage may occur. The corresponding expressions are

$$\frac{\delta_{out}}{X} = 0.38 \cdot \mathrm{Tu} \tag{A-7}$$

$$D_j = D_i \cdot \sqrt{\frac{V_i}{V_j}} \tag{A-8}$$

$$V_j = \sqrt{V_i^2 + 2gZ} \tag{A-9}$$

$$D_{out} = D_i + 2 \cdot \delta_{out} \cdot L \tag{A-10}$$

in which δ_{out} is the half angle of outer spread, *X* the longitudinal distance from the point of issuance, and *Z* the vertical fall distance of the jet. When using Equation (A-7), it is important to note that the angle δ_{out} is in degrees and *X* in meters.

The turbulence intensity Tu is dimensionless, expressed as a decimal. Typical outer angles of jet spread are 3% to 4% for rough turbulent jets (Ervine and Falvey 1987). The corresponding inner angles of jet spread are 0.5% to 1%. When investigating scour in practice, Tu is usually unknown. Under such circumstances, an estimation can be made based on the type of outlet structure (Table A-6, Bollaert 2002, 2004a).

This classification constitutes a simplification of reality. Tu may depend largely on specific geometric characteristics of the outlet, the flow pattern immediately upstream of the outlet, and so on. Whenever possible, all these aspects should be accounted for, and appropriate engineering judgment is necessary.

Furthermore, the angle of the jet at its point of impact is neglected in the present analysis, which is reasonable for impingement angles that are close to the vertical (70–90°). For smaller impingement angles, it is proposed to use the same hydrodynamic parameters as for vertical impingement but to redefine the water depth in the pool *Y* as the exact trajectory length of the jet through the water cushion and not as the vertical difference between water level and pool bottom.

Calculation of the other relevant variable when analyzing the plunging jet can be accomplished with Equations (A-8) to (A-10).

It is obvious that this module can be replaced by any type of turbulent flow structure that allows determining its main hydraulic and geometric characteristics (diameter, width, velocity, turbulence intensity). Types of flow already applicable are hydraulic jumps, vertical and horizontal river constrictions (abutments, sills, etc.), horizontal jet flows, etc. The module is actually being updated to account for bridge pier scour situations.

Plunge Pool Module

The second module refers to the hydraulic and geometric characteristics of the plunge pool downstream of the dam and defines the statistical characteristics of the hydrodynamic loading at the water–rock interface. The water depth *Y* in the plunge pool is an essential parameter of the scour model, because it defines the diffusion length of the impacting turbulent flow. During scour formation, the water depth *Y* has to be increased with the depth of the already formed scour *h.* Prototype observations indicate possible mounding at the downstream end of the pool. The mounding of rock results when the detached rock blocks are swept away and deposited immediately downstream. This can raise

Table A-6 Estimation of the Initial Jet Turbulence Intensity Tu Based on the Type of Outlet Structure (Bollaert 2002b)

Type of outlet	Tu
1. Free overfall	0–3 %
2. Ski-jump outlet	3–5 %
3. Intermediate outlet	3–8 %
4. Bottom outlet	3–8 %

the tailwater level. The effect is not described in the present model but can easily be added to the computations.

Knowledge of the water depth Y and the jet diameter at impact D_j (defined in the falling jet module) determines the ratio of water depth to jet diameter at impact Y/D_j. This ratio is directly related to diffusion characteristics of the jet.

The root-mean-square values of the pressure fluctuations at the water–rock interface, expressed by the C'_{pa} pressure coefficient, depend on the Y/D_j ratio and on the initial turbulence intensity Tu. Experimental data measured at near-prototype jet velocities (Bollaert 2002b) have been approximated by a polynomial regression (Eq. [12]) and are presented in Table A-7 for different turbulence intensity levels. Each curve corresponds to a degree of jet stability. The key issue is that Tu is considered to be fully representative of low-frequency instabilities of the jet. The curves are valid up to a Y/D_j ratio of 18 to 20. For higher ratios, the C'_{pa} value that corresponds to a ratio of 18 to 20 should be used. The range of values in Table A-7 is representative of the range of jet characteristics encountered in practice. Compact jets are smooth as they fall through the atmosphere, with no significant source of turbulence leading to low-frequency instability. Very turbulent jets are characterized by Tu values greater than 5%. In between these two outer bounds, other curves have been defined. They are applicable to low and moderately turbulent jets:

$$C_{pa} = 38.4 \cdot (1-\alpha_i) \cdot \left(\frac{D_j}{Y}\right)^2 \quad \text{for } Y/D_j > 4\text{–}6 \quad \text{(A-11)}$$

$$C_{pa} = 0.85 \quad \text{for } Y/D_j < 4\text{–}6 \quad \text{(A-12)}$$

$$\alpha_i = \frac{\beta}{1+\beta} \quad \text{(A-13)}$$

$$C'_{pa} = a_1 \cdot \left(\frac{Y}{D_j}\right) + a_2 \cdot \left(\frac{Y}{D_j}\right) + a_3 \cdot \left(\frac{Y}{D_j}\right) + a_4 \quad \text{(A-14)}$$

Table A-7 Polynomial Coefficients and Regression Coefficient for Different Turbulence Intensities of Jets (Bollaert 2002b; Bollaert & Schleiss 2005)

Tu [%]	a_1	a_2	a_3	a_4	Type of Jet
<1	0.000220	-0.0079	0.0716	0.000	Compact
1–3	0.000215	-0.0079	0.0716	0.050	Low turbulence
3–5	0.000215	-0.0079	0.0716	0.100	Moderate turbulence
>5	0.000215	-0.0079	0.0716	0.150	High turbulence

The nondimensional mean dynamic pressure coefficient C_{pa}, defined by Equations (A-11) to (A-13), decreases with increasing air content in the plunge pool and with increasing root-mean-square values of pressure fluctuation. The fluctuating dynamic pressure coefficient is calculated with Equation (A-14).

Similar to the falling jet module, any other type of turbulent flow impacting the water-rock interface can be used as input to the model, provided that the statistical parameters of the pressure fluctuations can be reasonably described (mean, RMS, extreme values).

Rock Mass Module

The plunge pool module defines the principal parameters of the hydrodynamic loading at the water-rock interface. This is used as input for determination of the hydrodynamic loading inside open- and closed-ended rock joints. The governing parameters are defined as (Fig. A-4, Bollaert 2002, 2004a)

1. maximum dynamic pressure coefficient $C_p^{\max}$
2. characteristic amplitude of pressure cycles Δp_c
3. characteristic frequency of pressure cycles f_c
4. maximum dynamic impulsion coefficient $C_I^{\max}$

The first parameter is relevant to brittle propagation (immediate failure) of closed-ended rock joints. The second and third parameters are used to calculate time-dependent failure (failure by fatigue) of closed-ended rock joints. The fourth parameter is used to define dynamic uplift of rock blocks formed by open-ended rock joints.

The maximum dynamic pressure coefficient $C_p^{\max}$ is obtained through multiplication of the root-mean-square pressure coefficient C'_{pa} with the amplification factor Γ^+ and by superposition with the mean dynamic pressure coefficient C_{pa}. The product of C'_{pa} times Γ^+ results in a pressure coefficient C^+_{pd}. The distinction between C_{pa} and C^+_{pd} is necessary because the amplification of the root-mean-square pressures influences only the fluctuating part of the dynamic pressures. As such, the maximum pressure value is written (Bollaert 2002) as

$$P_{\max}[\text{Pa}] = \gamma \cdot C_p^{\max} \cdot \frac{\phi \cdot V_j^2}{2g} = \gamma \cdot (C_{pa} + \Gamma^+ \cdot C'_{pa}) \cdot \frac{\phi \cdot V_j^2}{2g} \quad \text{(A-15)}$$

As a first approximation, the ϕ value for nonuniform velocity profiles is chosen equal to one. The main uncertainty of Equation (A-15) lies in the amplification factor Γ^+. Near-prototype scaled experiments resulted in the relationship for the amplification factors shown in Figure A-9.

The characteristic amplitude Δp_c of the pressure cycles is determined by the characteristic maximum and minimum pressures of the cycles. The minimum pressures are relatively constant and always close to standard atmospheric pressure. The maximum pressures are chosen equal to the $C_p^{\max}$ value.

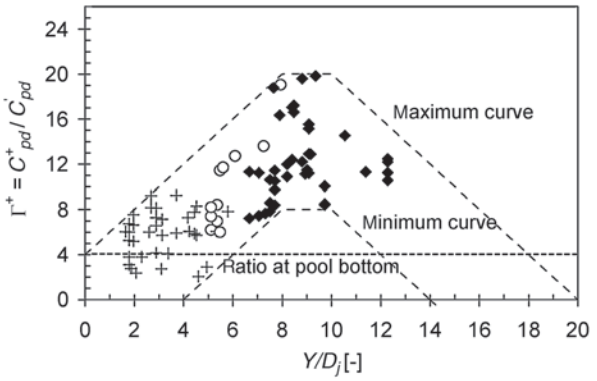

Fig. A-9. Amplification factor Γ^+ as a function of Y/D_j. The measured data are circumscribed by a maximum curve and a minimum curve, and represent core (+) and developed jet impact (♦) (Bollaert 2002).

The characteristic frequency of the pressure cycles f_c follows the assumption of a perfect open-closed resonator system and, thus, depends on the air concentration in the joint α_i and on the length of the joint L_f. The air content inside the joints can be directly related to the air content in the plunge pool (Bollaert and Schleiss 2003). This air content depends on the velocity of the jet at impact and on the plunge pool depth. The joint length depends on the distance between the different joint sets. For practice, a preliminary estimate of f_c can be made by assuming a mean celerity of 100 to 200 m/second (depending on the concentration of free air in the water) and joint lengths of typically 0.5 to 1 m. This results in frequencies of 25 to 100 Hz.

Besides the pressure loading inside the rock joints, the resistance of the rock to failure also has to be determined. The cyclic character of the pressure loading generated by the impact of a high-velocity jet on a closed-ended rock joint makes it possible to describe joint propagation by fatigue stresses occurring at the tip of the joint. This can be defined by linear elastic fracture mechanics (LEFM), assuming a perfectly linear elastic, homogeneous, and isotropic rock mass (Bollaert and Schleiss 2005). Despite these simplifying assumptions, its application to fractured rock becomes quite complicated when accounting for all the relevant parameters (Atkinson 1987; Whittaker et al. 1992; Andreev 1995).

Bollaert (2002, 2004a) developed a simplified methodology known as the comprehensive fracture mechanics (CFM) method for investigating rock scour that honors the underlying theory. Using this approach, pure tensile hydrodynamic loading inside rock joints is described by a stress intensity factor K_I. This parameter represents the amplitude of the rock mass stresses that are induced by the water pressures at the tip of the joint. The corresponding resistance to crack propagation offered by the rock mass is expressed by its fracture toughness K_{Ic}.

The challenge is to develop a comprehensive and physically representative implementation of the complex and dynamic conditions encountered in scour of fractured rock. Crack propagation distinguishes between brittle (or instantaneous) crack propagation and time-dependent crack propagation, subject to failure by fatigue. The former occurs when the stress intensity factor is equal to or greater than the fracture toughness of the material. The latter occurs when the maximum possible water pressure results in a stress intensity that is less than the material's resistance. Cracks can then be propagated by fatigue. Failure by fatigue depends on the frequency and the amplitude of the load cycles. The implementation of the fracture mechanics approach as it relates to hydrodynamic loading consists of a transformation of the water pressures σ_{water} in the joints into rock mass stresses at the joint end. The approach that was followed is based on the following simplifying assumptions: 1) the dynamic character of the loading has no influence, 2) the water pressure distribution inside the joints is constant, 3) only simple geometrical joint configurations are considered, and 4) joint surfaces are planar.

These stresses are characterized by the stress intensity factor K_I as follows:

$$K_I = P_{\max} \cdot F \cdot \sqrt{\pi \cdot L_f} \tag{A-16}$$

in which K_I is in MPa$\sqrt{m}$ and $P_{\max}$ in MPa. The boundary correction factor F depends on the type of crack and on its persistency, that is, its degree of cracking defined as a/B or b/W in Figure A-9. This figure presents three basic configurations for partially jointed rock, and simplifying assumptions are that the water pressure in the joints are assumed to be applied from outside, and no geometries with multiple joints are considered.

The choice of the most relevant geometry depends on the type and the degree of jointing of the rock. The first type of crack shown in Figure A-9 is of semielliptical or semicircular shape and, pertaining to the laterally applied water pressure $P_{\max}$, partially sustained by the surrounding rock mass in the two horizontal directions. As such, it is the geometry with the highest possible support of surrounding rock. Appropriate stress intensity factors should be used in case of low to moderately jointed rock. The second type of crack is a single-edged notch that is of a two-dimensional nature. Support from the surrounding rock mass is exerted only perpendicular to the plane of the notch, and, as a result, stress intensity factors will be substantially higher than for the first case. Thus, this crack type is relevant to significantly to highly jointed rock. The third geometry type is center cracked throughout the rock. Similar to the single-edge notch, only one-sided rock support can be accounted for. This support, however, should be slightly higher than that of the single-edged notch. The second and third configurations correspond to a partial destruction of the first one. They are more sensitive to stresses and have to be used for significant to highly jointed rock.

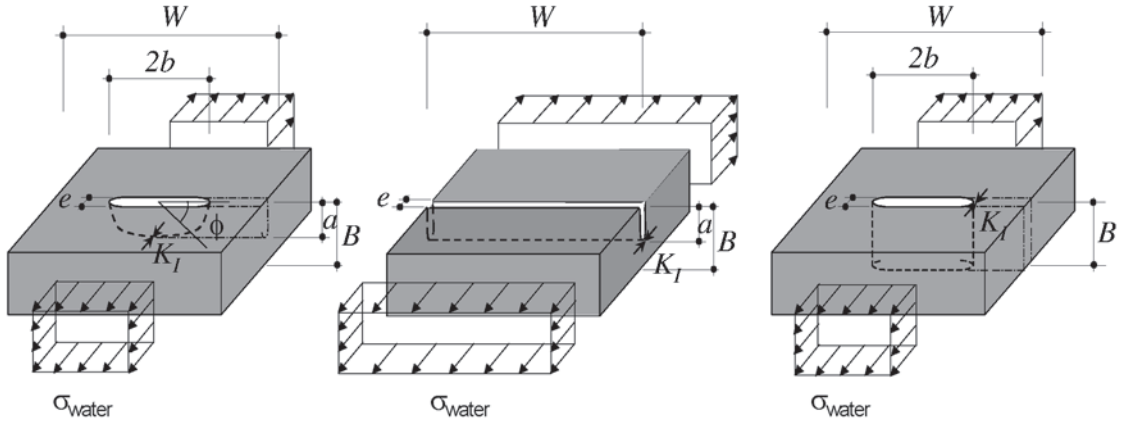

Fig. A-10. Main geometrical configurations of jointed rock: (a) semi-elliptical (EL) joint; (b) single edge (SE) joint; (c) center-cracked (CC) joint (Bollaert 2004a).

A summary of F values is presented in Figure A-10. For practical purposes, values of a/B of b/W greater than or equal to 0.5 are considered to correspond to completely broken-up rock; that is, the DI method is considered to be more applicable than the CFM method. For values of 0.1 or less, it is considered that a pure tensile strength approach is more plausible than a fracture mechanics approach. The F values for fissured rock where the CFM is assumed relevant are those associated with the range of a/B or b/W values between 0.20 and 0.40. This determination also depends on the type and number of joint sets, the degree of weathering, joint spacing, and so on.

The fracture toughness K_{Ic} depends on a wide range of parameters. Its determination has been simplified below by relating it to tensile strength T or unconfined compressive strength UCS and the in-situ stress field of the rock mass (σ_c). Based on a regression of data available in the literature,

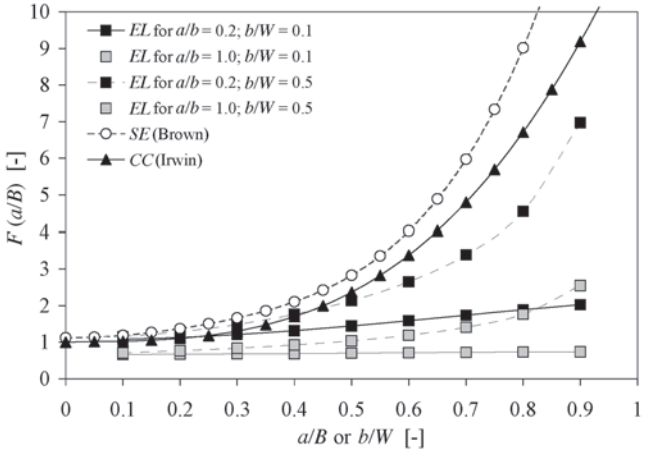

Fig. A-11. Comparison of different boundary correction factors F for the computation of the stress intensity at the tip of a rock joint (Bollaert 2004a).

the in-situ fracture toughness K_{Iins} can be defined as (Bollaert 2002):

$$K_{Iins,\,T} = (0.105 \text{ to } 0.132)\cdot T + (0.054\cdot\sigma_c) + 0.5276 \quad \text{(A-17)}$$

$$K_{Iins,\,UCS} = (0.008 \text{ to } 0.010)\cdot UCS + (0.054\cdot\sigma_c) + 0.42 \quad \text{(A-18)}$$

The units of T, UCS, and σ_c are expressed in MPa.

Instantaneous or brittle crack propagation will occur if

$$K_I \geq K_{I,ins} \quad \text{(A-19)}$$

If this is not the case, crack propagation is time dependent. This is expressed by an equation of the type originally proposed to describe fatigue crack growth in metals (Bollaert 2002, 2004a):

$$\frac{dL_f}{dN} = C_r \cdot (\Delta K_I / K_{Ic})^{m_r} \quad \text{(A-20)}$$

in which L_f is the joint length and N the number of pressure cycles. C_r and m_r are rock material parameters that can be determined by fatigue tests and, ΔK_I is the difference of maximum and minimum stress intensity factors at the joint tip. To implement time-dependent crack propagation into a comprehensive engineering model, the parameters m_r and C_r are summarized at Table A-8 for different rock types. First-hand calibration of these parameters resulted in an m_r value of 10 to 12 and a C_r value of 1E-07 for granite rock. Hence, while the m_r values can reasonably be used for practical purposes, the value of the C_r coefficients appears to be not as well defined. It could be one to two orders of magnitude higher than the theoretically proposed values in Table A-8.

The fourth hydrodynamic parameter is the maximum dynamic impulsion $C_I^{\max}$ in an open-end rock joint (underneath a rock block). This parameter is obtained by a time integration of the net forces on the rock block (Bollaert 2002, 2004a):

$$I_{\Delta tpulse} = \int_0^{\Delta tpulse} (F_u - F_o - G_b - F_{sh})\cdot dt = m\cdot V_{\Delta tpulse} \quad \text{(A-21)}$$

Table A-8 Fatigue Exponent m_r and Fatigue Coefficient C_r for Different Rock Types (Bollaert 2002b)

Type of Rock	Exponent m_r	Coefficient C_r
Arkansas novaculite	0.5	1.0E-8
Mojave quartzite	10.2–12.9	3.0E-10
Tennessee sandstone	4.8	4.0E-7
Solenhofen limestone	8.8–9.5	1.1E-8
Falerans micrite	8.8	1.1E-8
Tennessee marble	3.1	2.0E-6
Westerley granite	11.8–11.9	8.0E-10
Yugawara andesite	8.8	1.1E-8
Black gabbro	9.9–12.2	4.0E-9 to 5.0E-10
Ralston basalt	8.2	1.8E-8
Whin Sill dolerite	9.9	4.0E-9

in which F_u and F_o are the dynamic forces under and over the block, G_b is the immersed weight of the rock block, and F_{sh} represents the shear and interlocking forces. The shape of a block and the type of rock define the immersed weight of the block. The shear and interlocking forces depend on the joint pattern and the in-situ stresses. As a first approximation, they can be neglected by assuming that progressive dislodgment and opening of the joints occurred during the breakup phase of the rock mass. The pressure field over the block is governed by the turbulent shear layer of the jet. The pressure field under the block corresponds to transient pressure waves inside open-ended rock joints.

The pressures and forces are considered independent of block movement, which is a simplification of reality because shear and interlocking forces can vary considerably, depending on changes in block position and orientation. These forces depend on the points of contact between the blocks and on the in-situ horizontal stress field and are difficult to assess. Also, the pressure forces under the block may decrease because of the cavity that is formed once the latter starts moving. This, however, is difficult to formulate. As a firsthand approximation, the transient pressures under the block are assumed to be independent of the movement of the block. This seems plausible for a high peak pressure value during a small time interval but is less evident for lower pressures during a relatively long time period.

The first step is to define the instantaneous differences in forces over and under the block. By integrating the net uplift forces over a small time period Δt, the net impulsions I and a maximum net impulsion I^{max} can be obtained.

Second, I^{max} is made nondimensional by defining the impulsion as the product of a net force and a time period. For this, the net force is firstly transformed into a pressure. This means that the problem is solved for a unit surface area of the block (1 m^2 depending on the units). This pressure can then be made nondimensional by dividing it by the incoming kinetic energy $\phi \cdot V^2/2g$ as was done for the surface pressures. This results in a net uplift pressure coefficient C_{up}. The time period is made nondimensional by the travel period characteristic for pressure waves inside open-ended rock joints, that is, $T = 2 \cdot L_f/c$, in which L_f stands for the total joint length and c for the mean wave celerity. This results in a time coefficient T_{up}. Following this line of reasoning, a nondimensional impulsion coefficient C_I can be defined by the product $C_{up} \cdot T_{up} = V^2 \cdot L/g \cdot c$ [$m \cdot s$], presented in Figure A-12 as a function of Y/D_j.

The maximum net impulsion I^{max} is then obtained by multiplication of the value for C_I by $V^2 \cdot L/g \cdot c$. For jet velocities V_j greater than 20 m/second, a relatively constant value for C_I of 0.35 was observed during experiments (Bollaert 2002b). When expressed as a function of the Y/D_j ratio, the observable scatter is quite low. For core jets, a value of 0.6 to 0.8 seems plausible. For developed jets, the values are between 0.2 and 0.5. For practice, it is proposed to use the following polynomial expression:

$$C_I = 0.0035 \cdot \left(\frac{Y}{D_j}\right)^2 - 0.119 \cdot \left(\frac{Y}{D_j}\right) + 1.22 \qquad \text{(A-22)}$$

Failure of a rock block is then expressed by the displacement it undergoes due to the net impulsion (Eq. [A-21]). This kinetic energy is transformed into a net uplift displacement h_{up}. The displacement that is necessary to eject a rock block from its matrix is difficult to define. It depends on the degree of interlocking of the blocks, which depends on the in-situ stress field of the rock mass. A very tightly jointed rock mass will need a displacement that is equal to or higher than the height of the block. Less tightly jointed rock will probably be uplifted more easily. The necessary displacement is a model parameter that needs to be calibrated. Firsthand calibrations performed on the well-known Cabora-Bassa scour

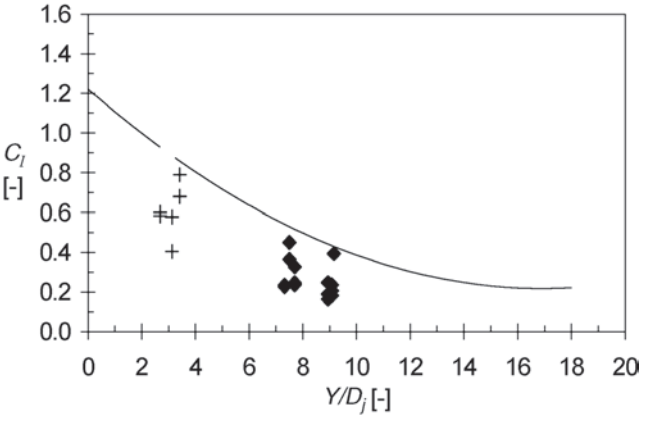

Fig. A-12. Non-dimensional impulsion for pressures inside open-end rock joints: CI as a function of Y/D_j; (Bollaert 2002).

case in Mozambique (Bollaert 2002) resulted in a necessary displacement equal to 0.20 times the block height.

SUMMARY

The current state-of-the-art in rock scour technology is represented by the EIM (Annandale 1995, 2006) and the CSM (Bollaert 2002, 2004a; Bollaert and Schleiss 2005). Both these methods can be used to determine scour thresholds and extent. However, the CSM offers the additional ability to calculate rate of scour, which is particularly relevant in the case of fissured media, such as rock, concrete of stilling basins or strongly cohesive soils. Also, the DI method incorporated into the CSM allows describing sudden failure of anchored concrete slabs of stilling basins (Bollaert 2004b).

Comprehensive descriptions, examples, and case studies demonstrating application of these methods to assess scour of rock and other earth and engineered earth materials are presented in Bollaert (2004b) for dynamic uplift of stilling basin concrete slabs, in Bollaert (2005), (2006), Bollaert et al. (2006) and Bollaert and Mason (2006) for time-dependent scour of rock in plunge pools, and in Annandale (2006) for applications of the EIM.

Theory and applications of most other existing methods to predict rock scour can be found in Schleiss and Bollaert (2002).

The EIM is based on an erosion threshold that is defined by relating the relative magnitude of the erosive capacity of water (expressed in terms of steam power) to the relative ability of rock to resist scour (expressed in terms of a geomechanical index known as the erodibility index). The scour threshold relationship can be used concurrently with estimates of the rate of change of stream power in scour holes, as they develop, to calculate the extent of scour.

The CSM addresses two failure modes of rock scour: scour of fissured rock and scour of jointed and fractured rock. In both cases, the erosive power of water is represented by pressure fluctuations that can easily be calculated in practice for plunging jets using methods proposed by Bollaert (2002, 2004a) and for any other type of turbulent flow whenever mean and fluctuating pressure values can be readily estimated. As an example, the method has already been applied to hydraulic jumps and is actually being extended towards scour of bridge piers founded in rock. The ability of rock to resist scour when using the CSM is determined by making use of LEFM approaches in the case of fissured rock and a force balance in the case of jointed and fractured rock. Fissured rock can fail by brittle fracture or in a time-dependent fashion in subcritical failure mode. In the case of brittle fracture, the stress intensity within a fissure exceeds its fracture toughness. Time-dependent failure is subject to the amplitude of pressure fluctuations and its frequency and the ability of the rock to withstand these forces to prevent fatigue failure. Dynamic impulsion of rock blocks occurs when net uplift pressures occur during a certain time interval. This impulsion method is also applicable to uplift of concrete slab linings.

Joint application of the EIM and CSM provides improved understanding of rock scour potential and extent. The geomechanical index used by the EIM provides a means to represent varying rock properties in an empirical manner using borehole and core data. It can be used to calculate scour potential and scour extent for varying flow conditions. The CSM uses basic fracture mechanics approaches and basic principles of physics to assess rock scour potential. In addition to providing the ability to assess scour threshold and extent, it can also be used to calculate the rate of rock scour. As such, it provides a much more detailed assessment of the phenomenon. A sound and complete parametric comparison of both models has been developed, allowing combined application in a fully consistent manner (Bollaert and Annandale 2004; Annandale and George 2006).

REFERENCES

Andreev, G. E. (1995). *Brittle failure of rock materials,* Balkema, Rotterdam, Brookfield.

Annandale, G. W. (1995). "Erodibility." *J. Hydr. Res.,* 33(4), 471–494.

Annandale, G. W. (2006). *Scour technology*, McGraw-Hill, New York.

Atkinson, B. K. (1987). *Fracture mechanics of rock,* Academic Press, London.

Bollaert, E.F.R. (2002). "The influence of plunge pool air entrainment on the presence of free air in rock joints." *Proc. of the Int. Workshop on Rock Scour,* EPFL, Lausanne, Switzerland, 137–149.

Bollaert, E.F.R. (2004a). A comprehensive model to evaluate scour formation in plunge pools. *Int. J. Hydropower & Dams*, 2004, 2004(1), pp. 94–101.

Bollaert, E.F.R. (2004b). A new procedure to evaluate dynamic uplift of concrete linings or rock blocks in plunge pools, *International Conference on Hydraulics of Dams and River Structures*, Teheran, Iran.

Bollaert, E.F.R. (2005). The Influence of Geomechanic and Hydrological Uncertainties on Scour at Large Dams: Case Study of Kariba Dam (Zambia-Zimbabwe). *73rd Annual ICOLD Meeting*, Tehran, Iran.

Bollaert, E.F.R. (2006). Physics Based Model Applied to Tucurui Dam (Brazil). *3rd Intl. Conference on Scour and Erosion*, Amsterdam, The Netherlands.

Bollaert, E. F. R., and Annandale, G. W. (2004, April). "Parametric comparison of erodibility index method and comprehensive scour model." *Int. Conference on Hydraulics of Dams and River Structures,* Tehran, Iran.

Bollaert, E.F.R. and Schleiss, A. (2003). Scour of rock due to the impact of plunging high velocity jets Part II: Experimental results of dynamic pressures at pool bottoms and in one-and two-dimensional closed end rock joints. *Journal of Hydraulic Research*, 41(5), 465–480.

Bollaert, E.F.R., and Schleiss, A. (2005). Physically based model for evaluation of rock scour due to high-velocity jet impact. *Journal of Hydraulic Engineering*, 131(3), 153–165.

Bollaert, E.F.R. and Mason, P.J. (2006). A Physically Based Model for Scour Prediction at Srisailam Dam. *Intl. Journal on Hydropower & Dams*, Issue 4, 96–103.

Bollaert, E.F.R., Vrchoticky, B. and Falvey, H.T. (2006). Extreme Scour Prediction at High-Head Concrete Dam and Stilling Basin (United States). *3rd Intl. Conf. on Scour and Erosion*, Amsterdam, The Netherlands.

Deere, D. U., and Deere, D. W. (1988). "The rock quality designation (RQD) index in practice." *Rock classification systems for engineering purposes: ASTM STP-984,* L. Kirkaldie, ed., American Society for Testing and Materials, Philadelphia, 91–101.

Emmerling, R. (1973). "The instantaneous structure of the wall pressure under a turbulent boundary layer flow," Report 56/1973, Gottingen, Germany, Max Planck Institute for Flow Research.

Ervine, D. A., and Falvey, H. R. (1987). "Behavior of turbulent jets in the atmosphere and in plunge pools." *Proc. of the Institution of Civil Engineers,* pt. 2, vol. 83, 295–314.

Ervine, D. A., Falvey, H. R., and Withers, W. (1997). "Pressure fluctuations on plunge pool floors." *J. Hydr. Res.,* 35(2), 257–279.

George, M., and Annandale, G. W. (2006). "Case study: Kariba Dam plunge pool scour." *Proc. Third Int. Conference on Scour,* Amsterdam.

Hinze, J. O. (1975). *Turbulence*, 2nd ed., New York, McGraw-Hill.

Kirsten, H. A. D. (1988). "Case histories of groundmass characterization for excavatability." *Rock classification systems for engineering purposes: ASTM, STP 984,* L Kirkaldie, ed., American Society for Testing and Materials, Philadelphia, 102–120.

Kirsten, H. A. D. (1982). "A classification system for excavation in natural materials." *The Civil Engineer in South Africa,* July, 292–308 (discussion in vol. 25, no. 5, May 1983).

Schleiss, A.J. and Bollaert, E.F.R. (2002). *Rock Scour due to Falling High-Velocity Jets*, A.A. Balkema Publishers, The Netherlands.

Whittaker, B. N., Singh, R. N., and Sun, G. (1992). *Rock fracture mechanics,* Elsevier, The Netherlands.